Journal of Marine Science and Application (2025) 24: 552-566
https://doi.org/10.1007/s11804-024-00459-6

RESEARCH ARTICLE

Improved Inverse First-Order Reliability Method for Analyzing Long-Term Response Extremes of Floating Structures

Junrong Wang[1], Zhuolantai Bai[1], Botao Xie[2], Jie Gui[1], Haonan Gong[1] and Yantong Zhou[1]

Received: 03 January 2024 / Accepted: 22 February 2024

Abstract

Long-term responses of floating structures pose a great concern in their design phase. Existing approaches for addressing long-term extreme responses are extremely cumbersome for adoption. This work aims to develop an approach for the long-term extreme-response analysis of floating structures. A modified gradient-based retrieval algorithm in conjunction with the inverse first-order reliability method (IFORM) is proposed to enable the use of convolution models in long-term extreme analysis of structures with an analytical formula of response amplitude operator (RAO). The proposed algorithm ensures convergence stability and iteration accuracy and exhibits a higher computational efficiency than the traditional backtracking method. However, when the RAO of general offshore structures cannot be analytically expressed, the convolutional integration method fails to function properly. A numerical discretization approach is further proposed for offshore structures in the case when the analytical expression of the RAO is not feasible. Through iterative discretization of environmental contours (ECs) and RAOs, a detailed procedure is proposed to calculate the long-term response extremes of offshore structures. The validity and accuracy of the proposed approach are tested using a floating offshore wind turbine as a numerical example. The long-term extreme heave responses of various return periods are calculated via the IFORM in conjunction with a numerical discretization approach. The environmental data corresponding to *N*-year structural responses are located inside the ECs, which indicates that the selection of design points directly along the ECs yields conservative design results.

Keywords Long-term response analysis; Floating structures; Inverse first-order reliability method; Convolution model; Gradient-based retrieval algorithm; Environmental contour method

1 Introduction

Marine structures experience various marine environments during their service. Therefore, ensuring structural reliability during the design phase is crucial. The engineering community usually adopts the response-based design method, which considers full long-term response analysis of structures as the design benchmark (Farnes and Moan, 1993; Naess and Moan, 2012). However, a full long-term response analysis, which requires a large amount of time domain simulations or model tests, is extremely cumbersome to be widely used. Hence, the calculation efficiency of the long-term response of marine structures is important in the design phase.

Inverse reliability methods are widely investigated in the field of offshore structures given their high efficiency and accuracy of structural long-term extreme-response analysis, i. e., inverse first-order reliability method (IFORM) based on the simple iterative algorithm (Li and Foschi, 1998) and exact arc search algorithm (Du et al., 2004).

The structure's *N*-year return period (RP) response can be obtained using convolution models in conjunction with a joint probability distribution model of environmental parameters, such as wave heights and periods (Sagrilo et al., 2011; Giske et al., 2017). Through the display of five common convolution models, Sagrilo et al. (2011) discussed

Article Highlights

- An improved gradient-based retrieval algorithm is proposed to solve convolution models via the inverse first-order reliability method.
- The improved algorithm has a fast convergence rate and avoids nonconvergence due to periodic oscillation.
- Environmental contours are used to describe wave conditions.
- With the use of discrete physical parameters, a numerical discretization integration approach is developed to extend the application scope of the convolution model.
- Long-term heave response in a floating offshore wind turbine is investigated to verify the improved algorithm and discretization integration approach.

✉ Botao Xie
xiebt@cnooc.com.cn

[1] College of Engineering, Ocean University of China, Qingdao 266100, China

[2] CNOOC Research Institute, Beijing 100027, China

model assumptions and their simplified forms and then proposed an improved method for the effective evaluation of long-term convolution integration via the combination of IFORM and importance sampling in Monte Carlo simulations. Giske et al. (2017) used two forms of IFORM to calculate the eigenvalues of the long-term extreme response of a structure; the calculation was simplified by reducing the number of evaluations of the limit state function, and a sufficient increase condition along with a backtracking approach is utilized to solve the failure of IFORM iteration to converge to the optimal point. Further, Chen et al. (2023) applied a convolution model algorithm with a good convergence to predict long-term extreme torsional moments in the connections of very large floating structures with two-directional hinges and mooring lines under random waves. For nonlinear marine structures under long-term response analysis (Farnes and Moan, 1993), Basrholm and Moan (2000) applied a linear analysis method based on contribution coefficients to identify important sea states for long-term response analysis in 2000; an acceptable estimation of the N-year RP response of the nonlinear system can be obtained through iterative analysis of a limited number of sea states.

The environmental contour method (ECM) is used in conjunction with the IFORM to design marine structures. Based on the environmental contour (EC) obtained using IFORM (Winterstein et al., 1993), short-term extreme responses can be determined under critical environmental conditions on the contour; thus, long-term extreme responses can be approximately obtained. The advantages of this method include the independent consideration of environmental loads for the response and the calculation of the response from a limited set of design sea conditions. For extreme statistical estimation related to complex response problems (Haver and Winterstein, 2008), the IFORM applies to the design case with specific annual exceedance probabilities, i.e., if a 100-year sea state is employed in the design, the expected maximum response will be evidently higher than the annual exceedance probability response. In addition, ECM is used to analyze complex responses of marine structures, such as the N-year mooring extreme tension of FPSO (Vázquez-Hernández et al., 2011; Fontaine et al., 2013), long-term response of a large-span pontoon bridge (Giske et al., 2018), the main girder jitter of Hardanger bridge (Lystad et al., 2020), and long-span bridges (Castellon et al., 2022). Compared with the full long-term response, the superiorities along with similarities and differences are demonstrated; Fontaine et al. (2013) also used this method to derive joint distribution extremes of ocean parameters (wave, wind, and current) for marine structural design. Studies on the applications of ECM, including the modified ECM (Li et al., 2017; Li et al., 2019; Beshbichi et al., 2022) and a novel ECM of a bivariate kernel density estimation approach (Wang, 2020), have become increasingly widespread. Moreover, Liao et al. (2022) proposed a three-dimensional (3D) IFORM-based approach that considers the short-term extreme response as the third variable and compared it with other EC building methods. Mackay and Hauteclocque (2023) presented a model-free method to estimate ECs in an arbitrary number of dimensions without the joint distribution of variables.

For the EC diagram, the marine environmental conditions should be described accurately, and the corresponding probability model must be established. The accuracy of probability distribution models under environmental conditions directly influences the prediction accuracy for structural long-term response. For structural analysis under wave action, the joint probability distribution models of considerable wave height and spectral peak period, univariate (Battjes, 1972; Longuet-Higgins, 1975) and bivariate probability functions (Haver, 1985), and covariate effect models (Ewans and Jonathan, 2014) have been studied. However, for the improved accuracy of the study, probability distribution models of environmental parameters for various sea areas must be statistically analyzed using measured data fitted with multiple distribution functions and established through the selection of the most appropriate probability function (Vanem, 2016; Bruserud et al., 2018; Clarindo and Guedes Soares, 2024).

Earlier studies indicated improvements in the existing long-term response convolution models. First, for the reduced number of iteration steps of the backtracking method, an improved retrieval algorithm based on gradient has been proposed; this algorithm ensures the accuracy of IFORM in solving the convolution model and improving the algorithm efficiency. Regardless, the application of the numerical discretization method extends to the applicability of the convolution integration model from a single-degree-of-freedom (SDOF) structure to an in-real complex floating structure. The rest of this paper is organized as follows: Section 2 briefly introduces the principle of IFORM and provides a summary of five long-term extreme-response convolution models. Section 3 investigates the long-term response of the SDOF structure under wave action. Section 4 iteratively solves the convolution model via IFORM and proposes a gradient-based optimal retrieval algorithm. Moreover, we expand this work to a floating offshore wind turbine (FOWT) and implement the numerical discretization approach to solve the structure's long-term response. Finally, Section 5 provides some conclusions.

2 Reliability theory and convolution models

In engineering applications, the establishment of the wave statistical model is accomplished by assuming the ocean surface as a random wave field with stationary and ergodic within a short period (e.g., 3–6 hours) and uniform in space.

Stationary random waves can be considered a random process with ergodicity, which can be deemed as an infinite superposition of microamplitude waves of different frequencies, amplitudes, and random phases.

Similarly, given the short-term stationary nature of environmental parameters, their associated loading effects can be represented by a stationary stochastic process, and their long-term stochastic variation can be described using the joint probability density function (PDF). Assuming the ergodicity of the long-term variation of environmental parameters and short-term loading processes, prediction of the long-term response can be made based on short-term response statistics. In practical engineering applications, the short-term response of a structure is usually evaluated via frequency or time domain analysis.

In this section, to solve the long-term response analysis of linear structures under wave action, we present convolution models based on three short-term response parameters, namely, all short-term response peaks, the extreme peak of short-term responses, and the zero-upcrossing rate of short-term responses. In this section, the principles and relationships of three different convolution models, along with their derivation, an approach to optimizing the convolution model, and reliability methods, are presented.

In addition, in this section, superscript $\tilde{X}$ represents the short-term characteristics of a parameter, and $\bar{X}$ represents its long-term characteristics.

2.1 Models based on all short-term peak responses

Assuming the statistical independence of short-term environmental parameters and response peaks for a certain short-term environmental condition, the probability that a single response peak R falls below a given level r in the long term can be defined as follows:

$$\begin{aligned} P(R \leqslant r) &= F_R(r) \\ &= P\left(R \leqslant r \middle| \boldsymbol{S} = \boldsymbol{s}_1\right) P\left(\boldsymbol{s}_1\right) + P\left(R \leqslant r \middle| \boldsymbol{S} = \boldsymbol{s}_2\right) \\ &\times P\left(\boldsymbol{s}_2\right) + \cdots + P\left(R \leqslant r \middle| \boldsymbol{S} = \boldsymbol{s}_{N_s}\right) P\left(\boldsymbol{s}_{N_s}\right) \end{aligned} \quad (1)$$

where $P\left(R \leqslant r \middle| \boldsymbol{S} = \boldsymbol{s}_i\right) = F_{R|\boldsymbol{S}}\left(r \middle| \boldsymbol{s}_i\right)$ refers to the cumulative conditional distribution of the global peak response for a given short-term condition. $P\left(\boldsymbol{s}_i\right)$ denotes the probability of an occurrence associated with a short-term condition $\boldsymbol{s}_i$, $P(R \leqslant r) = F_R(r)$ indicates the long-term peak response distribution, and N_s represents the expected number of short-term conditions over N years. Eq. (1) of the solution can be expressed as follows:

$$F_R(r) = \sum_{i=1}^{N_s} F_{R|\boldsymbol{S}}\left(r|\boldsymbol{s}_i\right) P\left(\boldsymbol{s}_i\right) = \int_{\boldsymbol{S}} F_{R|\boldsymbol{S}}(r|\boldsymbol{s}) f_{\boldsymbol{S}}(\boldsymbol{s}) \mathrm{d}\boldsymbol{s} \quad (2)$$

where $f_{\boldsymbol{S}}(\boldsymbol{s})$ corresponds to the joint PDF of the environmental parameters, and consideration of environmental conditions only applies to main wave parameters $\boldsymbol{S} = \left[\boldsymbol{H}_s, \boldsymbol{T}_p\right]$. Eq. (2) calculates the cumulative probability distribution (CDF) of the structural peak response below a given response r during an arbitrary short-term sea state. In the annual RP of the structure, the peak maximum response below r has the following CDF:

$$F_{R_N}(r) = \left[F_R(r)\right]^{\bar{v}_0 \tilde{T} N_S} = \left[\int_{\boldsymbol{S}} F_{R|\boldsymbol{S}}(r|\boldsymbol{s}) f_{\boldsymbol{S}}(\boldsymbol{s}) \mathrm{d}\boldsymbol{s}\right]^{\bar{v}_0 \tilde{T} N_S} \quad (3)$$

This model is denoted as A_1, where $\tilde{T}$ indicates the short-term duration, and $\bar{v}_0$ represents the corresponding long-term average zero-upcrossing rate:

$$\bar{v}_0 = \int_{\boldsymbol{S}} v_0(\boldsymbol{s}) f_{\boldsymbol{S}}(\boldsymbol{s}) \mathrm{d}\boldsymbol{s} \quad (4)$$

where v_0 refers to the average zero-upcrossing rate for the structural response during an arbitrary short-term environmental condition $\boldsymbol{S}$. This model is widely used as it is easily solved via structural reliability analysis. However, it ignores the different numbers of structural response peaks under various short-term sea conditions.

To prevent the error caused by model A_1; that is, the neglect of the different numbers of structural response peaks for each short-term sea state, we use the following model for calculations:

$$F_{R_N}(r) = \left[F_R(r)\right]^{\bar{v}_0 \tilde{T} N_S} = \left[\int_{\boldsymbol{S}} \frac{v_0(\boldsymbol{s})}{\bar{v}_o} F_{R|\boldsymbol{S}}(r|\boldsymbol{s}) f_{\boldsymbol{S}}(\boldsymbol{s}) \mathrm{d}\boldsymbol{s}\right]^{\bar{v}_0 \tilde{T} N_S} \quad (5)$$

This model is the most widely used method for long-term structural response analysis and is denoted as A_2.

2.2 Models based on the maximum peak of short-term response

Two long-term structural response analysis models based on all response peaks are presented in the above sections. Another approach is the application of structural response extremes at each short-term sea state as variables to determine the CDF of the long-term structural response. Considering the distribution of structural response extremes for a given short-term sea state, we obtain the following:

$$F_{R_e|\boldsymbol{S}}\left(r|\boldsymbol{s}\right) = \left[F_{R|\boldsymbol{S}}\left(r|\boldsymbol{s}\right)\right]^{v_0(\boldsymbol{s})\tilde{T}} \quad (6)$$

Then, the short-term response extreme peaks of CDF can be written as follows:

$$F_{R_e}(r) = \int_{\boldsymbol{S}} F_{R_e|\boldsymbol{S}}\left(r|\boldsymbol{s}\right) f_{\boldsymbol{S}}(\boldsymbol{s}) \mathrm{d}\boldsymbol{s} \quad (7)$$

Assuming the statistical independence of all short-term response extreme peaks, the CDF of structural long-term response extremes can be determined as follows:

$$\begin{aligned} F_{R_N}(r) &= \prod_{i=1}^{N_s} F_{R_e|\boldsymbol{S}}\left(r|\boldsymbol{s}_i\right) \\ &= \left(\exp\left(\int_{\boldsymbol{S}} \ln\left(F_{R|\boldsymbol{S}}(r|\boldsymbol{s})\right)^{v_0(\boldsymbol{s})\tilde{T}} f_{\boldsymbol{S}}(\boldsymbol{s})\mathrm{d}\boldsymbol{s}\right)\right)^{N_s} \end{aligned} \tag{8}$$

Krogstad (1985) and Ochi (1998) used this model (denoted as model B_1) in extreme wave height analysis. If the expectation $\bar{F}_{R_e}(r)$ of the long-term extreme distribution is utilized to approximate $\tilde{F}_{R_e}(r)$, then the structural short-term extreme distribution can be computed as follows:

$$\begin{aligned} F_{R_N}(r) &= \left(F_{R_e}(r)\right)^{N_s} = \left(\int_{\boldsymbol{S}} F_{R_e\boldsymbol{S}}(r|\boldsymbol{s}) f_{\boldsymbol{S}}(\boldsymbol{s})\mathrm{d}\boldsymbol{s}\right)^{N_s} \\ &= \left(\int_{\boldsymbol{S}} \left[F_{R|\boldsymbol{S}}(r|\boldsymbol{s})\right]^{v_0(\boldsymbol{s})\tilde{T}} f_{\boldsymbol{S}}(\boldsymbol{s})\mathrm{d}\boldsymbol{s}\right)^{N_s} \end{aligned} \tag{9}$$

Another model (denoted as model B_2) can be solved efficiently through the combination of structural reliability methods.

2.3 Model based on short-term response zero-upcrossing rate

Given ergodic environmental parameters, Naess (1984) expressed the long-term response extreme value distribution for the N-year RP of the structure as follows:

$$F_{R_N}(r) = \exp\left(-T\int_{\boldsymbol{S}} v_R(r|\boldsymbol{s}) f_{\boldsymbol{S}}(\boldsymbol{s})\mathrm{d}\boldsymbol{s}\right) \tag{10}$$

where $v_R(r|\boldsymbol{s})$ refers to the average-upcrossing rate r of structural response under ambient conditions $\boldsymbol{s}$. T denotes the long-period duration, $T = \tilde{T} \times N_s$. Their model is denoted as model C.

2.4 Reliability theory

Reliability methods are usually used in the analyis of structural reliability index or failure probability. For reliability problems, the transformation of reliability can simplify the problem considerably. The reliability formula $G_r(\boldsymbol{v})$ of the structural limit state function can be expressed as

$$G_r(\boldsymbol{v}) = r - \tilde{r} \tag{11}$$

where V means a random variable of the joint PDF $f_V(\boldsymbol{v})$, r denotes a given response level, and $\tilde{r}$ indicates the structural response value. When $G_r(\boldsymbol{v}) < 0$, the structure experiences failure. The probability of structural failure p_f describing the reliability problem can be determined as follows:

$$p_f = \int_{G(\boldsymbol{v}) \leqslant 0} f_V(\boldsymbol{v})\mathrm{d}\boldsymbol{v} \tag{12}$$

For convolution model B_2, the short-term extreme-response distribution function Eq. (9) can be rewritten in reliability form:

$$\begin{aligned} \bar{F}_{\tilde{R}}(r) &= \int_{\boldsymbol{S}} F_{\tilde{R}|\boldsymbol{S}}(r|\boldsymbol{s}) f_{\boldsymbol{S}}(\boldsymbol{s})\mathrm{d}\boldsymbol{s} \\ &= \int_{\boldsymbol{S}}\int_{\tilde{r} \leqslant r} f_{\tilde{R}|\boldsymbol{S}}(\tilde{r}|\boldsymbol{s})\mathrm{d}\tilde{r} f_{\boldsymbol{S}}(\boldsymbol{s})\mathrm{d}\boldsymbol{s} \end{aligned} \tag{13}$$

A random variable V is defined to be a set of environmental conditions $\boldsymbol{S}$ and structural responses $\tilde{\boldsymbol{R}}$, i.e., $V = \left[\boldsymbol{S}, \tilde{\boldsymbol{R}}\right]$. The joint PDF can be expressed as follows:

$$f_V(\boldsymbol{v}) = f_{R_e|\boldsymbol{S}}(\tilde{r}|\boldsymbol{s}) f_{\boldsymbol{S}}(\boldsymbol{s}) \tag{14}$$

Through substitution of the above equation into Eq. (13), we obtain the following:

$$\bar{F}_{\tilde{R}}(r) = \int_{\tilde{r} \leqslant r} f_V(\boldsymbol{v})\mathrm{d}\boldsymbol{v} = 1 - \int_{r-\tilde{r} \leqslant 0} f_V(\boldsymbol{v})\mathrm{d}\boldsymbol{v} \tag{15}$$

Substitution of Eq. (11) into Eq. (15), the following equation is acquired:

$$\bar{F}_{\tilde{R}}(r) = 1 - \int_{G_r(\boldsymbol{v}) \leqslant 0} f_V(\boldsymbol{v})\mathrm{d}\boldsymbol{v} = 1 - p_f(r) \tag{16}$$

At this point, we establish the connection between the extreme-response distribution function of model B_2 and failure probability. In determining the failure probability $p_f(r)$ corresponding to a given exceedance level r in Eq. (16), calculation usually involves the use of FORM. Random vector V is transformed into an independent standard normal variable $\boldsymbol{u} = \mathrm{trans}(\boldsymbol{V})$ using Rosenblatt transform, i.e., data are transformed from the physical parameter space (the space defined by $\boldsymbol{H}_s$, $\boldsymbol{T}_z$, and $\tilde{\boldsymbol{R}}$) into a standard normal space.

$$\begin{aligned} \Phi\left(\boldsymbol{u}_1\right) &= F_{\boldsymbol{H}_s}\left(\boldsymbol{H}_s\right) \\ \Phi\left(\boldsymbol{u}_2\right) &= F_{\boldsymbol{T}_z|\boldsymbol{H}_s}\left(\boldsymbol{T}_z|\boldsymbol{H}_s\right) \\ \Phi\left(\boldsymbol{u}_3\right) &= F_{R_e|\boldsymbol{H}_s,\boldsymbol{T}_z}\left(\tilde{\boldsymbol{R}}|\boldsymbol{H}_s,\boldsymbol{T}_z\right) \end{aligned} \tag{17}$$

where $\Phi(\boldsymbol{u})$ indicates the standard normal distribution function. Given that the functions involved are all CDF, i.e., monotonically increasing functions, transformation transpires in a two-way manner between a point in the standard normal space and the corresponding point in the physical parameter space. Given a point $\left(u_1, u_2, u_3\right)$ in the standard normal space, inverse Rosenblatt can be used to determine the corresponding point $\left(h_s, t_z, \tilde{r}\right)$ in the physical parameter space. The inversion process is completed as follows:

$$\begin{aligned} h_s(\boldsymbol{u}) &= F_{\boldsymbol{H}_s}^{-1}\left(\Phi\left(u_1\right)\right) \\ t_z(\boldsymbol{u}) &= F_{\boldsymbol{T}_z|\boldsymbol{H}_s}^{-1}\left(\Phi\left(u_2\right)|h_s(\boldsymbol{u})\right) \\ \tilde{r}(\boldsymbol{u}) &= F_{\tilde{\boldsymbol{R}}|\mathbf{H}_s,\mathbf{T}_z}^{-1}\left(\Phi\left(u_3\right)\middle| h_s(\boldsymbol{u}), t_z(\boldsymbol{u})\right) \end{aligned} \tag{18}$$

The probability of failure in standard normal space can be rewritten as the equation below:

$$p_f(r) = \int_{G(\boldsymbol{v})\leqslant 0} f_{\boldsymbol{V}}(\boldsymbol{v})\mathrm{d}\boldsymbol{v} = \int_{g(\boldsymbol{u})\leqslant 0} f_{\boldsymbol{U}}(\boldsymbol{u})\mathrm{d}\boldsymbol{u} \tag{19}$$

The converted limit state function is computed as follows:

$$g(\boldsymbol{u}) = r - \tilde{r}(\boldsymbol{u}) \tag{20}$$

In the transformed standard normal space, the corresponding probability density decreases with the increase in radius. The failure boundary in the physical parameter space $G_r(\boldsymbol{v})\leqslant 0$ is transformed into a standard normal space via Rosenblatt transformation, and the design point, which is expressed by the coordinate $\left(\hat{u}_1, \hat{u}_2, \hat{u}_3\right)$, refers to the point on the failure boundary closest to the origin. The distance from the design point to the origin is as follows:

$$\beta = \sqrt{\hat{u}_1^2 + \hat{u}_2^2 + \hat{u}_3^2} \tag{21}$$

In the FORM, the failure boundary is replaced by a tangent plane at the design point in standard normal space. In addition, given the rotational symmetry of multivariate standard normal distribution, the FORM-estimated failure probability can be expressed as follows:

$$p_f(r) = \int_{g(\boldsymbol{u})\leqslant 0} f_{\boldsymbol{u}}(\boldsymbol{u})\mathrm{d}\boldsymbol{u} = \Phi(-\beta) \tag{22}$$

Combining Eq. (16) with Eq. (22), we obtain the following:

$$F_{R_e}(r) \approx 1 - \Phi\left(-\beta\right) \tag{23}$$

When FORM assumes a small probability of failure, regardless of the nonlinearity of the limit state function $g(\boldsymbol{u})$ in the standard normal space, Eq. (22) still holds. FORM evaluates structural reliability at a given response level r. However, at a designated time, the response level of a structure corresponding to a certain exceedance probability, such as solving for the response extreme r_N of the structure for N-year RP, must be calculated. This response level is usually computerd using the annual exceedance probability of $1/N$, such as $F_{R_N}(r_M)=1-1/M$. Moreover, the extreme values of the N-year response can be expressed in short-term extreme distribution using Eq. (9) :

$$F_{R_e}\left(r_M\right) = \left(1 - \frac{1}{N}\right)^{1/M} \approx 1 - \frac{1}{N \times M} \tag{24}$$

where M refers to the number of short-term $\tilde{T}$ in a year, e.g., short-term cycle $\tilde{T}$ equals 3 hours, which corresponds to $M=24\times 365/3=2\,920$. The exceedance probability corresponding to the 100-year RP response extreme r_{100} of the structure is $1-F_{R_e}\left(r_{100}\right)=1/292\,000$. Given the exceedance probability corresponding to the response extreme, the reliability index β can be obtained using Eq. (22).

3 Numerical analysis of the convolution model via IFORM

The convolution model refers to the full long-term analysis method, and it applies relevant elements of the probabilistic model of environmental parameters. In consideration of complex structures or a large number of environmental conditions (e.g., wind speed, wave height, period, and current velocity), the calculation process of the above model becomes time-consuming and tedious. Therefore, the inverse reliability method for approximating the extreme value of long-term structural responses is proposed to simplify the solution of the convolution model. This section involves iteratively solving model B_2 via IFORM and proposes a novel retrieval method.

3.1 Improved gradient-based retrieval algorithm

To determine the design point, we need to find a value r_N to obtain $g_{r_N}(u)=r_N-\tilde{r}(\boldsymbol{u})=0$; that is, the problem is converted into solving a point on the sphere of radius β that maximizes $\tilde{r}(\boldsymbol{u})$ in standard normal space (Winterstein et al., 1993; Li and Foschi, 1998):

$$\begin{cases} r_N = \text{maxmize}\,\tilde{r}(\boldsymbol{u}) \\ \text{subject to}\,|\boldsymbol{u}| = \beta \end{cases} \tag{25}$$

For the problem in Eq. (25), the Lagrange multiplier method implies that the optimal point $\boldsymbol{u}^*$ must satisfy the following conditions:

$$\frac{\boldsymbol{u}^*}{\left|\boldsymbol{u}^*\right|} = \frac{\nabla\tilde{r}\left(\boldsymbol{u}^*\right)}{\left|\nabla\tilde{r}\left(\boldsymbol{u}^*\right)\right|} \tag{26}$$

Li and Foschi (1998) proposed an algorithm to solve Eq. (25) via IFORM calculation in the manner $\left|\boldsymbol{u}^*\right|=\beta$:

$$u^{k+1} = \beta\frac{\nabla\tilde{r}\left(\boldsymbol{u}^k\right)}{\left|\nabla\tilde{r}\left(\boldsymbol{u}^k\right)\right|} \tag{27}$$

The iteration in Eq. (27) is simple and convenient to apply. However, when the structural function is nonconcave, nonconvex, or with a high degree of nonlinearity, the method may suffer from periodic oscillations, which results

in the nonconvergence of iterations. As shown in Figure 1, the current iteration point is $\boldsymbol{u}^k$, and its gradient $\nabla\tilde{r}\left(\boldsymbol{u}^k\right)$ refers to the direction of local maximum rise near this point. In consideration of the iteration in Eq. (27), the vector $\boldsymbol{u}^{k+1}$ of a new verification point is parallel to $\nabla\tilde{r}\left(\boldsymbol{u}^k\right)$. When the gradient $\boldsymbol{u}^{k+1}$ at the new iteration point parallels vector $\boldsymbol{u}^k$, i.e., $\boldsymbol{u}^{k+2}$ coincides with $\boldsymbol{u}^k$, this iteration falls into periodic oscillations and shows no convergence.

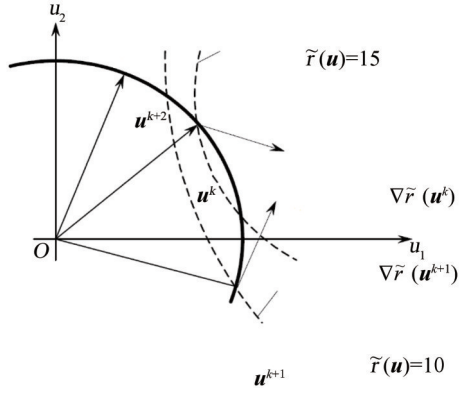

Figure 1 Schematic of the convergence problem

To solve this convergence problem, Giske et al. (2017) used an adequate growth condition and the backtracking method and minimized the evaluations of the functional function to simplify operations. The extreme value forecast results of the method were labeled as $\tilde{r}_N^{\mathrm{I}}$, and the frequency of calculating $\tilde{r}(\boldsymbol{u})$ is n^{I}. This method requires the proportionality of the increase in $\tilde{r}(\boldsymbol{u})$ to the step size when the iteration point is updated from $\boldsymbol{u}^k$ to $\boldsymbol{u}^{k+1}$ be and time derivative of $\boldsymbol{u}^k$ along the retrieval direction. In this example, the following equation is satisfied using $\boldsymbol{u}^{k+1}$:

$$\tilde{r}\left(\boldsymbol{u}^{k+1}\right)-\tilde{r}\left(\boldsymbol{u}^k\right)\geqslant cd\alpha \tag{28}$$

where $c\in(0,1)$, and $c=0.000\,1$. d indicates the directional derivative at the iteration point $\boldsymbol{u}^k$, and α denotes the distance between points $\boldsymbol{u}^k$ and $\boldsymbol{u}^{k+1}$.

$$d=\frac{1}{\beta}\sqrt{\beta^2\left|\nabla\tilde{r}\left(\boldsymbol{u}^k\right)\right|^2-\left(\boldsymbol{u}^k\cdot\nabla\tilde{r}\left(\boldsymbol{u}^k\right)\right)^2} \tag{29}$$

$$\alpha=\beta\cos^{-1}\frac{\boldsymbol{u}^k\cdot\nabla\tilde{r}\left(\boldsymbol{u}^k\right)}{\beta\left|\nabla\tilde{r}\left(\boldsymbol{u}^k\right)\right|} \tag{30}$$

Further, the method calculates the optimal step size once per iteration, which adds to the tediousness of the computation and increases the number of iterative steps. Thus, an improved gradient-based retrieval algorithm is proposed. Based on the gradient of iteration points, a fixed step is used to retrieve design points, i.e., a 1D retrieval algorithm is applied in the selection of iteration points on the sphere arc along the direction of the gradient of the kth iteration point without calculating the optimal step size for each iteration:

$$\boldsymbol{u}^{k+1}=\beta\frac{\boldsymbol{u}^k+d\dfrac{\nabla\tilde{r}\left(\boldsymbol{u}^k\right)}{\left|\nabla\tilde{r}\left(\boldsymbol{u}^k\right)\right|}}{\left|\boldsymbol{u}^k+d\dfrac{\nabla\tilde{r}\left(\boldsymbol{u}^k\right)}{\left|\nabla\tilde{r}\left(\boldsymbol{u}^k\right)\right|}\right|} \tag{31}$$

$\tilde{r}_N^{\mathrm{II}}$ represens the extreme value forecast result of the method, and the number of times $\tilde{r}(\boldsymbol{u})$ is referred to as n^{II}. The specific steps are as follows:

S1: Set the initial iteration step d, $k=0$, $\boldsymbol{u}^0=\left[\beta,0,0\right]$, and set convergence accuracy $\varepsilon=0.001$;

S2: Calculate $v_3\left(\boldsymbol{u}^k\right)$ and $\nabla v_3\left(\boldsymbol{u}^k\right)$;

S3: Select a new iteration point as follows: $\boldsymbol{u}^{k+1}=\beta\dfrac{\boldsymbol{u}^k+d\dfrac{\nabla\tilde{r}\left(\boldsymbol{u}^k\right)}{\left|\nabla\tilde{r}\left(\boldsymbol{u}^k\right)\right|}}{\left|\boldsymbol{u}^k+d\dfrac{\nabla\tilde{r}\left(\boldsymbol{u}^k\right)}{\left|\nabla\tilde{r}\left(\boldsymbol{u}^k\right)\right|}\right|}$;

S4: Calculate $\tilde{r}\left(\boldsymbol{u}^{k+1}\right)$;

S5: If $\tilde{r}\left(\boldsymbol{u}^{k+1}\right)-\tilde{r}\left(\boldsymbol{u}^k\right)>0$, proceed to S6. Otherwise, make $d=d/2$, and proceed to S3;

S6: If $\dfrac{\left|\boldsymbol{u}^{k+1}-\boldsymbol{u}^k\right|}{\left|\boldsymbol{u}^{k+1}\right|}<\varepsilon$, then proceed to S7. Otherwise, $k=k+1$, and proceed to S2;

S7: $k=k+1$, and the extreme of the N-year response of the structure is $\tilde{r}_N^{\mathrm{II}}=\tilde{r}\left(\boldsymbol{u}^k\right)$.

Figure 2 shows the iterative process in $\boldsymbol{u}$ space, with the initial iteration step including $d=1.4$ and $\boldsymbol{V}=\left[\boldsymbol{S},\tilde{\boldsymbol{R}}\right]=\left[\boldsymbol{H}_s,\boldsymbol{T}_z,\tilde{\boldsymbol{R}}\right]$, given a point in a standard normal space named $\boldsymbol{u}=\left[u_1,u_2,u_3\right]$, which corresponds to a point in the physical parameter space $\boldsymbol{v}=[\,h(\boldsymbol{u}),t(\boldsymbol{u}),\tilde{r}(\boldsymbol{u})\,]=\mathrm{trans}^{-1}(\boldsymbol{u})$:

$$\begin{aligned}
&h(\boldsymbol{u})=F_{\boldsymbol{H}_s}^{-1}\left(\Phi\left(u_1\right)\right)=\alpha\left[-\ln\left(1-\Phi\left(u_1\right)\right)\right]^{1/\beta}\\
&t(\boldsymbol{u})=F_{\boldsymbol{T}_z|\boldsymbol{H}_s}^{-1}\left(\Phi\left(u_2\right)\middle|\,h(u)\right)=\exp\left\{\mu(h(\boldsymbol{u}))+\sigma(h(\boldsymbol{u}))u_2\right\}\\
&\tilde{r}(\boldsymbol{u})=F_{\tilde{\boldsymbol{R}}|\boldsymbol{T}_z,\boldsymbol{H}_s}^{-1}\left(\Phi\left(u_3\right)\middle|\,h(\boldsymbol{u}),t(\boldsymbol{u})\right)=\sqrt{-2m_0(h(\boldsymbol{u}),t(\boldsymbol{u}))\ln\left(-\frac{2\pi}{\tilde{T}}\sqrt{\frac{m_0(h(\boldsymbol{u}),t(\boldsymbol{u}))}{m_2(h(\boldsymbol{u}),t(\boldsymbol{u}))}}\ln\Phi\left(u_3\right)\right)}
\end{aligned} \tag{32}$$

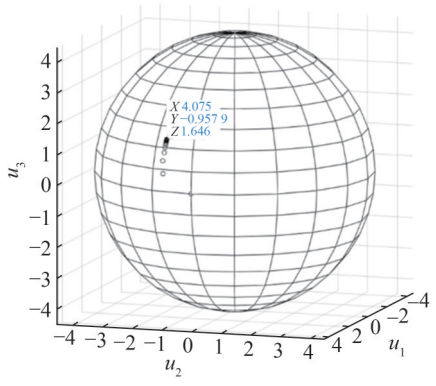

Figure 2 Iterative process of the improved gradient-based retrieval algorithm

3.2 SDOF and environmental model

Based on the above method, the long-term response of the SDOF model is subjected to numerical analysis. The response amplitude operator (RAO) of SDOF is assumed to be as follows:

$$H_{\eta R}(\omega) = \frac{1}{\left(\left(1 - \left(\frac{\omega}{\omega_n}\right)^2\right)^2 + \left(2\xi\frac{\omega}{\omega_n}\right)^2\right)^{1/2}} \tag{33}$$

where ω refers to the natural frequency, and ξ represents the damping ratio of the model. Under the assumption of linearity, the structure for a given short-term condition $\boldsymbol{S} = \left[\boldsymbol{H}_s, \boldsymbol{T}_p\right]$ exhibits the following response spectrum:

$$S_{R|\boldsymbol{S}}(\omega\,|\boldsymbol{s}) = \left|H_{\eta|R}(\omega)\right|^2 S_{\eta|\boldsymbol{S}}(\omega\,|\boldsymbol{s}) \tag{34}$$

where $S_{\eta|\boldsymbol{S}}(\omega\,|\boldsymbol{s})$ corresponds to the wave spectrum under the short-term condition $\boldsymbol{S} = \boldsymbol{s}$, and the P-M wave spectrum is given as follows:

$$\begin{aligned}\boldsymbol{S}_{\eta|S}(\omega|\boldsymbol{s}) &= \boldsymbol{S}_{\eta|\boldsymbol{H}_s,\boldsymbol{T}_z}(\omega|h_s,t_z)\\ &= \frac{h_s^2 t_z}{8\pi^2}\left(\frac{\omega t_z}{2\pi}\right)^{-5}\exp\left\{-\frac{1}{\pi}\left(\frac{\omega t_z}{2\pi}\right)^{-4}\right\}\end{aligned} \tag{35}$$

The sea surface is a smooth Gaussian stochastic process, and thus, an SDOF structure exhibits a stochastic response that is likewise a Gaussian stochastic process. The narrow-band process involves a short-term structural response that obeys the Rayleigh distribution model:

$$F_{R|\boldsymbol{S}}(r|\boldsymbol{s}) = 1 - \exp\left(-\frac{r^2}{2m_0(\boldsymbol{s})}\right) \tag{36}$$

The average zero-upcrossing rate of the response under the short-term condition $\boldsymbol{S}=\boldsymbol{s}$ is as follows:

$$v(r|\boldsymbol{s}) = \frac{1}{2\pi}\sqrt{\frac{m_2(\boldsymbol{s})}{m_0(\boldsymbol{s})}}\exp\left(-\frac{r^2}{2m_0(\boldsymbol{s})}\right) \tag{37}$$

where m_i denotes the ith order moment of the response spectrum:

$$m_i(\boldsymbol{s}) = \int_0^\infty \omega^i \boldsymbol{S}_{R|\boldsymbol{S}}(\omega\,|\boldsymbol{s})\mathrm{d}\omega \tag{38}$$

In this section, the same environmental model of the North Sea indicated in the work of Giske et al. (2017) is used. According to their paper, Weibull distribution describes the long-term distribution of a significant wave height $\boldsymbol{H}_s$, and zero-crossing period $\boldsymbol{T}_z$ obeys log-normal distribution under $\boldsymbol{H}_s$ conditions. Thus, the joint probability distribution of environmental parameters can be computed as follows:

$$\begin{aligned}f_{\boldsymbol{H}_s\boldsymbol{T}_z}(h,t) &= f_{\boldsymbol{H}_s}(h)\,f_{\boldsymbol{T}_z|\boldsymbol{H}_s}(t|h)\\ f_{\boldsymbol{H}_s}(h) &= \frac{\beta}{\alpha}\left(\frac{h}{\alpha}\right)^{\beta-1}\exp\left\{-\left(\frac{h}{\alpha}\right)^{\beta}\right\}\\ f_{\boldsymbol{T}_z|\boldsymbol{H}_s}(t|h) &= \varphi\left(\frac{\ln t - \mu(h)}{\sigma(h)}\right)\end{aligned} \tag{39}$$

The parameters $\alpha=1.76$ and $\beta=1.59$ of the Weibull distribution are fitted. The smoothing parameter curve of the log-normal distribution is fitted as follows:

$$\begin{aligned}\mu(h) &= a_0 + a_1 h^{a_2}\\ \sigma(h) &= b_0 + b_1 e^{b_2 h}\end{aligned} \tag{40}$$

Table 1 provides all the associated parameters, and Figure 3 displays the ECs of 10-, 100-, and 1 000-year RPs accordingly.

Table 1 Parameters of the fitted smoothing function

i	a_i	b_i
0	0.70	0.07
1	0.282 0	0.344 9
2	0.167 0	−0.207 3

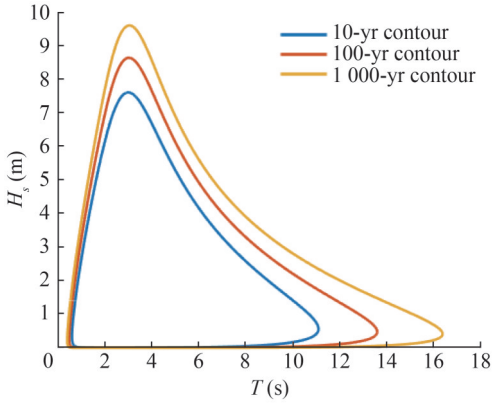

Figure 3 $H_s - T_z$ ECs of different RPs

3.3 Numerical analysis

In this section, numerical analysis is performed for SDOF at various natural frequencies. The long-term extreme responses of this SDOF are investigated using six different sets of natural frequencies ω_n=1.0, 1.5, 2.0, 2.5, 4.0, 6.0 rad/s, and damping ratio ξ= 0.05. Figure 4 shows the corresponding RAOs.

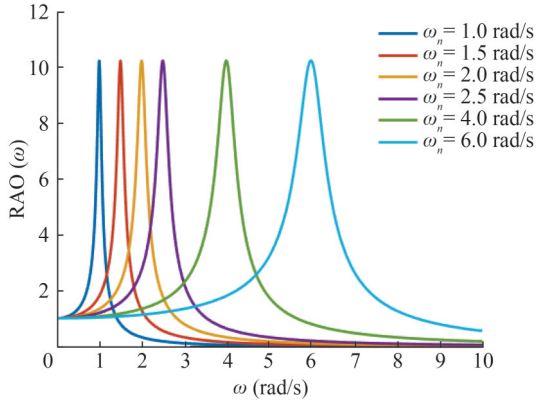

Figure 4 RAOs of different SDOF models at various frequencies

To compare the differences between the five convolutional models intuitively, we show in Tables 2 and Table 3 the long-term response results of the five models calculated via convolutional integration under different RPs.

Table 2 10-year RP extreme response of the SDOF model

ω_n (rad/s)	A_1	A_2	B_1	B_2	C
1.0	27.67	26.97	26.97	25.73	26.97
1.5	36.11	35.95	35.95	34.60	35.95
2.0	35.38	35.44	35.44	34.20	35.44
2.5	31.53	31.68	31.67	30.57	31.67
4.0	20.89	21.18	21.14	20.24	21.14
6.0	13.42	13.79	13.78	12.95	13.78

Table 3 100-year RP extreme response of the SDOF model

ω_n (rad/s)	A_1	A_2	B_1	B_2	C
1.0	31.86	31.06	31.04	30.41	31.04
1.5	41.25	40.99	40.69	40.30	40.69
2.0	40.25	40.17	40.17	39.58	40.17
2.5	35.79	35.85	35.84	35.30	35.84
4.0	23.74	23.97	23.90	23.48	23.90
6.0	15.35	15.70	15.69	15.16	15.69

Approximate model A_1 overestimates or underestimates long-term response extremes with respect to three exact models because it is based on the average of all short-term peaks of the response and disregards the number of peaks of the resulting response in each short-term condition. In addition, its deviation depends on structural properties. By contrast, model B_2, which is based on average short-term extreme peaks, usually underestimates the long-term response extremes of a structure, and its deviation depends on structural dynamic characteristics. In addition, differences in the forecasting results of the long-term convolution model are mainly related to the modeling approach and not to the joint probability model used for environmental parameters. Thus, if other joint probability distribution models of environmental parameters are employed in the same long-term response analysis, the same similarities and differences in the calculated results should be observed.

In the long-term response analysis of SDOF in this example, the calculated result of model A_1 achieves an error of 0.049%–2.69% compared with the exact model, and the error of approximate model B_2 reaches 0.20%–6.09% compared with model A_1. Evidently, in this case, the relative errors of the two approximation methods for the calculation of long-term response extremes of the structure are not significant. However, convolution model A_1 yields more accurate results model B_2. Both approximation models are suitable for combination with structural reliability methods to achieve rapid integration method solutions. For practical complex structures, numerical evaluation of integration is tedious and time-consuming, and the use of approximate models for fast solutions with IFORM is preferred.

The long-term extremes calculated via IFORM of the five models under sea conditions and two retrieval methods are used in iterations. Tables 4 and 5 show the results of 10- and 100-year RPs, respectively.

Table 4 Long-term response of the SDOF structure (10-year RP)

ω_n (rad/s)	r_N	$\tilde{r}_N^{\mathrm{I}}$	$\tilde{r}_N^{\mathrm{II}}$	δ (%)	n^{I} (Giske's)	n^{II} (This paper)
1.0	26.97	27.27	27.36	1.46	64	20
1.5	35.95	35.94	36.04	0.25	59	20
2.0	35.44	35.30	35.39	−0.14	38	20
2.5	31.67	31.45	31.54	−0.42	37	20
4.0	21.14	20.71	20.79	−1.65	27	20
6.0	13.78	12.94	13.01	−5.58	37	27

Table 5 Long-term response of the SDOF structure (100-year RP)

ω_n (rad/s)	r_N	$\tilde{r}_N^{\mathrm{I}}$	$\tilde{r}_N^{\mathrm{II}}$	δ (%)	n^{I} (Giske's)	n^{II} (This paper)
1.0	31.04	31.83	31.88	2.70	75	21
1.5	40.69	41.48	41.53	2.06	54	21
2.0	40.17	40.54	40.59	1.04	38	21
2.5	35.84	36.07	36.11	0.76	37	21
4.0	23.90	23.96	24.00	0.43	38	21
6.0	15.69	15.34	15.39	−1.91	48	27

In Tables 4–5, r_N represents the exact result of the long-term response obtained via convolutional integration, and the approximate values, $\tilde{r}_N^{\mathrm{I}}$ and $\tilde{r}_N^{\mathrm{II}}$, are the two solutions by IFORM, with a relative error $\delta = \dfrac{\tilde{r}_N^{\mathrm{II}} - r_N}{r_N} \times 100\%$, and n^{I} and n^{II} are the numbers of calculated $\tilde{r}(\boldsymbol{u})$. With respect to the exact result, the error δ of the IFORM estimates r_N ranges between −6.12%–3.01%. Therefore, IFORM can be considered in obtaining a reasonable prediction of the extreme value r_N of the structural response. In addition, the gradient-based retrieval algorithm proposed in this paper solves the IFORM problem with a considerable reduction in the evaluations of the function n^{II} compared with n^{I} in the work of Giske et al. (2017). The improved algorithm based on IFORM can substantially increase the solution speed of calculation while avoiding the problems of oscillation and nonconvergence during iteration. In addition, the number of iterations ranges between 30%–70% of that of the comparison model, which reduces the computational complexity of the long-term response analysis of the structure considerably, especially for complex offshore structures.

4 Long-term linear response analysis of floating structures

4.1 Limitations of the applicability of the convolution model

The above-mentioned research is mainly used to solve the SDOF via convolutional integration or IFORM, whose limitation is having an SDOF with an idealized structure and no practical engineering significance, which leads to its limited applicability and nonfeasibility in practical engineering analysis. In addition, the convolutional analysis method is based on known RAO expressions, which are substituted into the convolutional model for calculations. However, for general floating structures with a complex hull shape, their RAO curves lack a specific analytic formula, which prevents the use of the convolutional integral model. When the response RAOs are insolvable, the convolutional model must be extended to complex offshore structures. Therefore, this section will introduce a numerical discretization method to expand the application of the study.

4.2 Numerical discretization method

To address the limitations of the convolutional analysis, this paper proposes the discretization of parameters to solve the nonparsability of the convolutional model with multiple degrees of freedom. To ensure that the calculation can be performed, the frequency, RAO, and environment parameters should have identical numbers of discretization to ensure that each scatter corresponds to a seriatim calculation. Therefore, the condition for method implementation is the assurance that the same number of discrete parameters will be used. The method discretizes the RAO curve to form a scatter matrix to approximate the amplitude. Correspondingly, the wave and response spectra are also discretized by the same amount. Figure 5 shows the solution flowchart of this method.

The detailed solution steps of this method include the following:

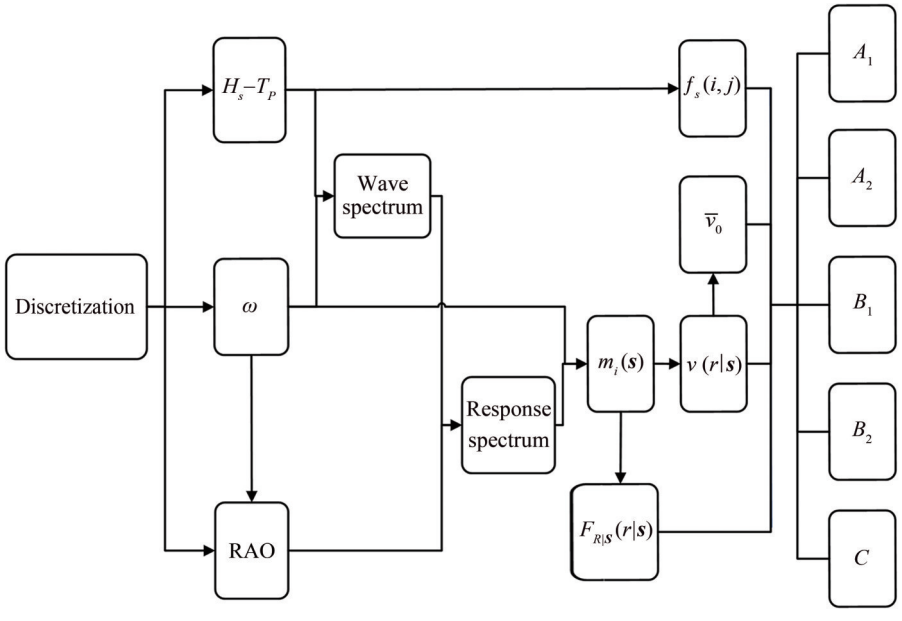

Figure 5 Flow chart of numerical discretization method

1) Determine the discretization range and number N_d of wave frequency ω, discretize ω into a vector $\omega(i)$, and interpolate the RAO to obtain the discretized RAO data vector RAO(ω). Furthermore, discretize environmental parameter surface $H_s - T_p$ using the same size of $N_d \times N_d$ to obtain the discrete joint probability distribution model;

2) Substitute the values of environmental parameters and $\omega(i)$ into Eq. (35), which corresponds to the scatter matrix of the wave spectrum, and combine RAO (ω) to obtain the response spectrum scatter according to Eq. (34);

3) According to Eq. (38), the spectral moment $m_i(\boldsymbol{s})$ is determined using the discrete integration form for the response spectral function with respect to ω. Then, the extreme value distribution $F_{R|\boldsymbol{S}}(r|\boldsymbol{s})$ of the structural short-term response is obtained using Eq. (36);

4) In turn, the structural short-term zero-upcrossing rate $v_0(\boldsymbol{s})$ and long-term average zero-upcrossing rate $\bar{v}_0$ are acquired, and the iterative solution of the convolution model in the framework of IFORM can be applied using the above-obtained parameters.

4.3 Analyzed example: A semisubmersible FOWT

To verify the feasibility and accuracy of the method above, we analyze an FOWT located in the South China Sea as an example. Based on the discretization method, the platform's long-term response extremes are computed through convolutional integration and IFORM, respectively, and the calculated results are compared and verified.

Table 6 lists the main particulars of the FOWT. The hydrodynamic wet surface model is established (Figure 6). Table 6 and Figure 7 provide the relevant parameters and schematic of its mooring system, respectively. The frequency domain hydrodynamic parameters are calculated using DNV WADAM, and the obtained heave RAO is shown in Figure 8.

Table 6 Main particulars of the FOWT platform

Column side length (m)	12
Column center distance (m)	76
Column height (m)	28
Pontoon height (m)	5
Float tank diameter (m)	31
Draft (m)	14.5
Displacement (m)	13 000
Depth of water (m)	65
Diameters of mooring chain (m)	0.122/0.208
Mooring radius (m)	450
Mooring pretension (kN)	774.7

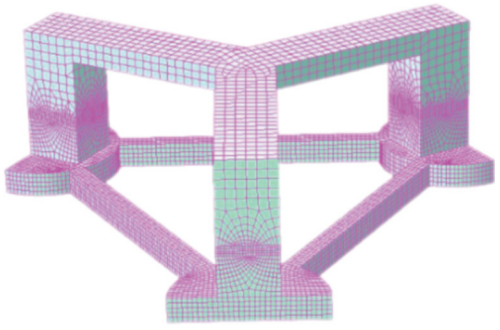

Figure 6 Wet surface model of the FOWT platform

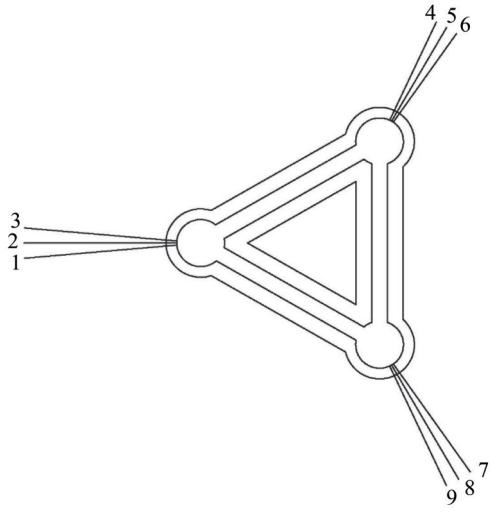

Figure 7 Diagram of the mooring system

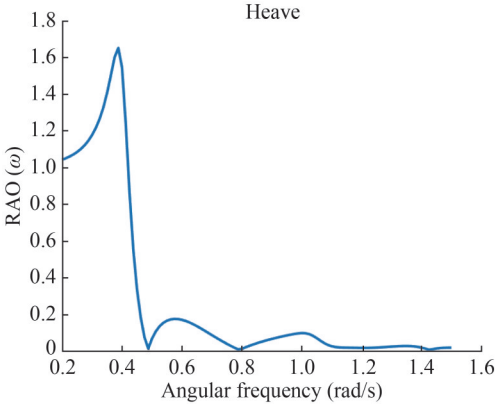

Figure 8 Heave RAO of the FOWT

In terms of environmental modeling, based on 40 years worth of wave simulation data on the South China Sea, significant wave height H_s and spectral peak period T_p are selected as two-dimensional environmental parameters. A structural probability distribution model of $H_s - T_p$ is obtained using maximum likelihood estimation in MATLAB. The joint probability distribution model of Weibull-generalized extreme value is used to describe the joint probability distribution of $H_s - T_p$ with the following expressions:

$$f_{H_s}(h)=\frac{\beta}{\alpha}\left(\frac{h}{\alpha}\right)^{\beta-1}\exp\left\{-\left(\frac{h}{\alpha}\right)^{\beta}\right\}$$

$$f_{T_p|H_s}(t|h)=\frac{1}{\sigma(h)}\left[1+k\left(\frac{x-\mu(h)}{\sigma(h)}\right)\right]^{-\frac{1}{k(h)^{-1}}}\exp\left\{\left[1+k\left(\frac{x-\mu(h)}{\sigma(h)}\right)\right]^{-\frac{1}{k(h)}}\right\} \tag{41}$$

$$f_{H_sT_p}(h,t)=f_{H_s}(h)f_{T_p|H_s}(t|h)$$

The model parameters are fitted to the following smoothing function:

$$\begin{aligned}k(h)&=C=0.037\,86\\ \mu(h)&=a_1+a_2h^{a_3}\\ \sigma(h)&=b_1+b_2e^{b_3h}\end{aligned} \tag{42}$$

Table 7 shows the parameters used to fit the smoothing function in the above equation.

Table 7 Parameters of the fitted smoothing function

i	a_i	b_i
1	4.591	0.425 2
2	2.121	0.818 1
3	0.679 3	−0.400 0

According to the above probability distribution model, the joint probability ECs of H_s-T_p under 10-, 100-, and 1 000-year RPs are obtained via the IFORM, and the results are shown in Figure 9.

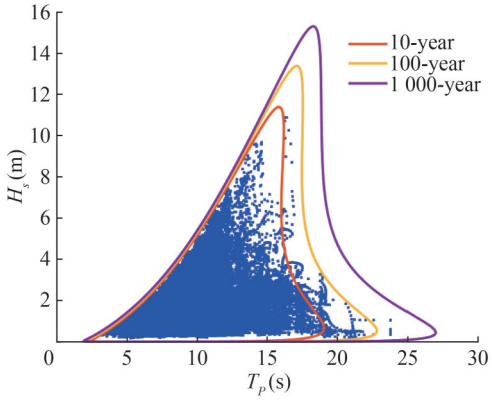

Figure 9 H_s-T_p ECs in the south china sea

4.4 Discretization

For the application of the convolution model in complex structures, the RAO and environmental parameters must be discretized before they can be applied to the solution. The structural heave RAO is interpolated. Then, discretization of the wave spectrum and environmental parameters is performed using a fixed number of scattered points within a sufficient length interval and calculated using the scattered integral after one-to-one correspondence.

According to Eq. (38), solving for response spectral moments involves the integration of the response spectrum with respect to the wave frequency ω from 0 to positive infinity. However, the discretization process is finite, and thus, a large range should be selected to ensure the accuracy of calculation results. After structural hydrodynamic analysis, RAO magnitude $<10^{-5}$ at $\omega\geqslant 5$, which is ignorable. Thus, the frequency range (0, 5) is selected. Then, interpolation of the RAO curve yields a discrete vector of size N_d ($N_d=488$ here), which is noted as $\omega(k)$ and RAO(k), where k is an integer and takes the value range of $[1,N_d]$.

Similarly, H_s and T_p are discretized to the vectors of size N_d. Based on the EC plotted in Figure 9, the selected discretization range of H_s approximates (0,20), and the discretization step spans 0.04 m to obtain H_s vector as $H_s(i)$. In addition, T_p is discretized within a period range of (0, 30) with a discretization step of 0.06 s to determine the discretized vector $T_p(j)$. Here, i and j are integers belonging to the interval of $[1,N_d]$.

Substitution of $\omega(k),H_s(i),T_p(j)$ into Eq. (35) solves the discrete matrix of the wave spectrum. Combined with the discrete point RAO(k), the response spectrum discrete matrix is obtained using Eq. (34). According to Eq. (38), the zero-order moment $m_0(i,j)$ and second-order moment $m_2(i,j)$ are solved through the integration of response spectrum function with respect to ω.

As displayed in Eq. (37), $r=0$ represents the zero-upcrossing rate of structural short-term response at a certain sea state $\boldsymbol{S}=\boldsymbol{s}$. After the substitution of $m_0(i,j)$ and $m_2(i,j)$, the scattered values of the zero-upcrossing rate of the short-term response at various sea states, which is the discrete form of v_0, are denoted as $v_0(i,j)$.

For the environment model, based on the 1D discrete data $H_s(i)$ and $T_p(j)$, the square matrix $h_s(i,j)$ and $t_p(i,j)$ of size $N_d\times N_d$ (488×488) is constructed, and the discrete joint PDF $f_{H_sT_p}(h_s(i,j),t_p(i,j))$, briefly denoted as $f_s(i,j)$, is obtained through the combination of the constructed environment model Eq. (41).

Therefore, discrete data are obtained, and the scattered points, whose size is related to the size of H_s or T_p, form a grid between them. Figures 10–13 show the grid representations of response spectral moments $m_0(i,j)$ and $m_2(i,j)$, H_s-T_p discrete PDF $f_s(i,j)$, and the short-term zero-upcrossing rate of the structure $v_0(i,j)$, respectively.

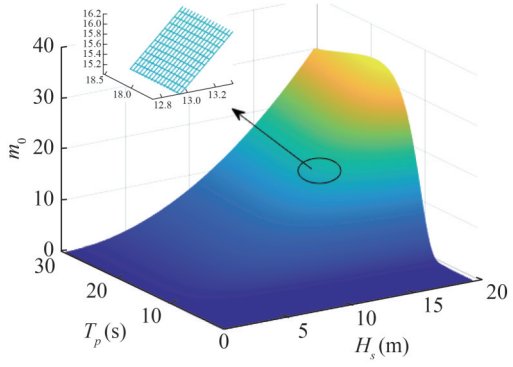

Figure 10 Gridded zero-order response spectrum moments

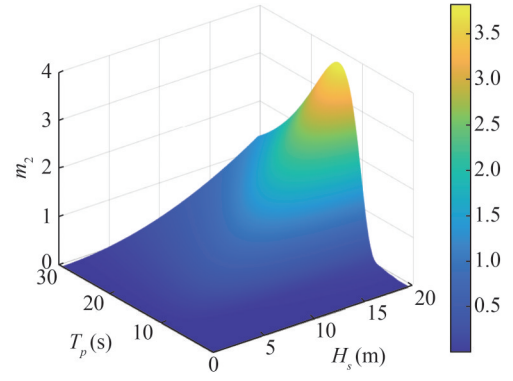

Figure 11 Gridded second-order response spectrum moments

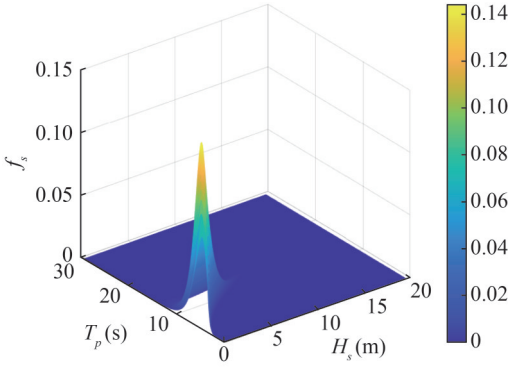

Figure 12 Joint PDF of $H_s - T_p$

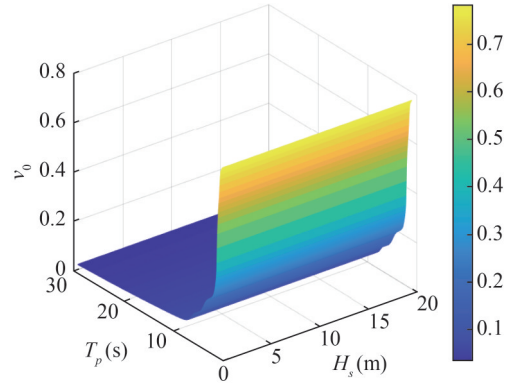

Figure 13 Short-term zero-upcrossing rate

The long-term zero-upcrossing rate of a structure refers to the surface integration of the short-term zero-upcrossing rate over all sea conditions (h_s, t_p), i.e., the volume of the spatial body formed by solving the 3D surface of the short-term average zero-upcrossing rate and $H_s - T_p$ plane. Based on the 3D grid diagram in Figure 12, the concept of splitting and superposition is performed, each grid is treated as a cell, and the volume of each cell is approximated and accumulated to obtain the total volume in space. Through approximation of the space enclosed by the surface cells and coordinate planes as a square, the square volume can be computed using the product of the centroid height of each grid cell and grid area. Then, Eq. (4) is rewritten in a discrete form:

$$\bar{v}_0 = A \sum_{i=1}^{N_d - 1} \sum_{j=1}^{N_d - 1} v_{0\text{int}}(i, j) f_s(i, j) \tag{43}$$

where A refers to the cell grid area, and $v_{0\text{int}}(i, j)$ denotes the average zero-upcrossing rate of each grid centroid in $v_0(i, j)$.

4.5 Solving the long-term heave response of FOWT

4.5.1 By convolutional integration

The above discrete model reveals that the long-term response of three convolution models, B_1, B_2, and C, are solved via convolutional integration based on structural heave RAO to evaluate long-term response extremes under different RPs. The final calculation results are shown in Table 8.

Table 8 *N*-year RP heave response of the FOWT platform

Return period	B_1	B_2	C
10-year	13.62	13.05	13.62
100-year	15.98	15.68	15.98

As mentioned before, models B_1 and C are various forms of the same long-term convolution model, and they can be obtained via mathematical approximation transformations. Then, the long-term heave response of the floating platform of three different RPs is solved through the application of the numerical discrete method. Models B_1 and C show perfect agreement. The results by model B_2, which are based on average short-term extremes, are smaller than those by models B_1 and C, which tend to underestimate long-term response extremes. The calculated results verify the effectiveness of the proposed discretization approach.

4.5.2 By IFORM

Based on the discrete model above, model B_2 is solved

via IFORM discrete iterations and validated against the convolution integration results.

The definition of failure probability in Eq. (22) serves as the basis for determining the structure's reliability index:

$$\beta = -\Phi^{-1}\left(-\ln\left[1-\frac{1}{MN}\right]\right) \tag{44}$$

where M represents the total annual sea state, N denotes the design RP, and β is calculated as shown in Table 9.

In the sphere delineating the reliable domain in standard normal space, the initial iteration point is (0, 0, β). This iteration step d is set as 1.4, and each point in the iterative process $\boldsymbol{u} = (u_1, u_2, u_3)$ corresponds to $\boldsymbol{v} = \left(h(\boldsymbol{u}), t(\boldsymbol{u}), \tilde{r}(\boldsymbol{u})\right)$ in the real physical parameter space. The coordinates of the iteration point can be written based on the joint probability distribution of the environmental parameters in subsection 4.3:

$$\begin{aligned} h(\boldsymbol{u}) &= F_{H_s}^{-1}\left(\Phi(u_1)\right) = \alpha\left[-\ln\left(1-\Phi(u_1)\right)\right]^{1/\beta} \\ t(\boldsymbol{u}) &= F_{T_s|H_s}^{-1}\left(\Phi(u_2)\middle|h(\boldsymbol{u})\right) = \frac{\left[-\ln\left(\Phi(u_2)\right)\right]^{-C-1}}{C\sigma(h(\boldsymbol{u}))+\mu(h(\boldsymbol{u}))} \\ \tilde{r}(\boldsymbol{u}) &= F_{R|T_z,H_s}^{-1}\left(\Phi(u_3)\middle|h(\boldsymbol{u}),t(\boldsymbol{u})\right) = \sqrt{-2m_0(h(\boldsymbol{u}),t(\boldsymbol{u}))\ln\left(-\frac{2\pi}{\tilde{T}}\sqrt{\frac{m_0(h(\boldsymbol{u}),t(\boldsymbol{u}))}{m_2(h(\boldsymbol{u}),t(\boldsymbol{u}))}}\ln\Phi(u_3)\right)} \end{aligned} \tag{45}$$

This example involves the use of the improved gradient-based retrieval algorithm proposed in Section 3.1 in obtaining the solution, and the iteration accuracy tolerance is set as 0.001. Figure 14 shows a schematic of the iterative solution using IFORM for the 10-year RP. After 18 iterations of retrieval, the extreme value of $\tilde{r}(\boldsymbol{u})$ is obtained from the initial point in the standard normal space with the coordinates of (3.84, 0.07, 1.05). In addition, the coordinates of data returned to the physical parameter space are (10.88, 15.52, 13.08), which means a long-term response extreme $\tilde{r}(\boldsymbol{u})$ of 13.08 m at H_s= 10.88 m and T_p= 15.52 s.

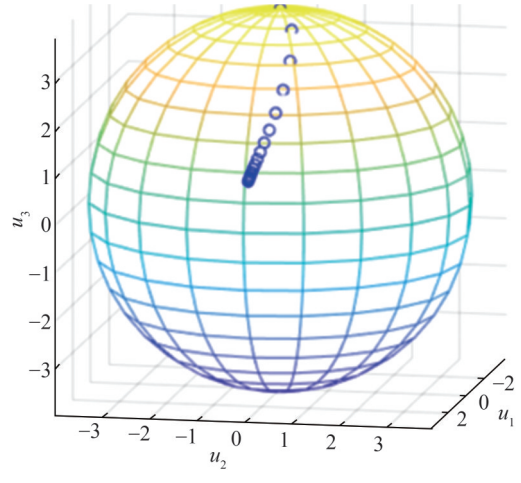

Figure 14 Schematic of the IFORM iterative process

Table 10 shows the computed results of IFORM and their comparison with the findings of convolution integration for different RPs, where r_N denotes the convolution integration result of model B_2, r_{NI} indicates that of the IFORM-solving model B_2, δ refers to the relative error between the two outcomes, which is defined as $\delta = \frac{r_{NI}-r_N}{r_N}\times 100\%$, and n is the number of iterations. The relative errors δ are all within 0.3%, and δ are less than 0.1% in 100- and 1 000-year RP cases (Table 10). In this sense, the discretization IFORM method can provide accurate solution results. In addition, the number of iteration steps of the gradient-based retrieval method n is reduced compared with the method used by Giske et al. (2017); moreover, the value of iteration step d can be adjusted to reduce the iteration steps and shorten the convergence period.

Table 9 Reliability indexes for N-year RPs

10-year	100-year	1 000-year
3.982	4.498	4.966

Table 10 Comparisons of heave by convolutions integration and IFORM approaches

Return period	r_N	r_{NI}	δ	n
10-year	13.05	13.08	0.23%	18
100-year	15.68	15.69	0.06%	19
1 000-year	18.25	18.26	0.05%	19

Table 11 provides the coordinates retrieved via iterations in the standard normal space and the corresponding coordinates in the physical parameter space, and Figure 15 shows the plot of the corresponding extreme sea states in the ECs. In general, a minor difference is observed between the improved gradient-based retrieval algorithm and the method proposed by Giske et al. (2017). The environmental condition design point obtained using the improved algorithm is located inside the EC, which indicates that this method may be more economical than the EC method, especially for long RPs.

Table 11 Final retrieval points and corresponding sea state

Return period	(u_1, u_2, u_3)	$(h(\boldsymbol{u}), t(\boldsymbol{u}), \tilde{r}(\boldsymbol{u}))$
10-year	(3.84, 0.07, 1.05)	(10.88, 15.52, 13.08)
100-year	(4.26, 0.04, 1.46)	(12.44, 16.53, 15.69)
1 000-year	(4.60, 0.02, 1.86)	(13.82, 17.39, 18.26)

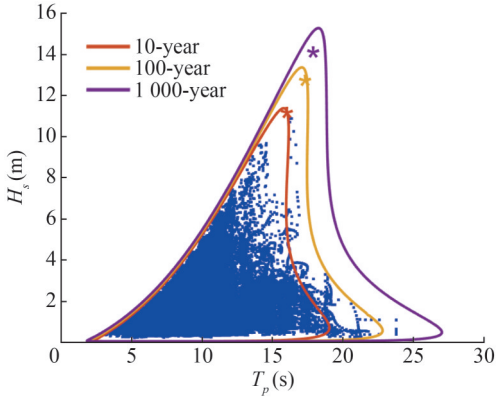

Figure 15 Extreme sea state points corresponding to *N*-year

5 Conclusions

This paper has proposed an improved IFORM for the analysis of long-term response extremes of floating structures. Five long-term response convolution models are initially demonstrated and analyzed. These models are used to investigate the long-term response of the SDOF structure under waves. A modified gradient-based retrieval algorithm is proposed to solve the long-term convolution models in the IFORM framework. The modified algorithm can effectively prevent the non-onvergence problem due to periodic oscillations and requirement of fewer iterations than when using the sufficient increase condition and backtracking method.

In addition, a numerical discrete integration method is developed through the combination of an improved gradient-based retrieval algorithm for the calculation of long-term responses of a floating structure in which RAO cannot be analytically expressed. The heavy long-term response of a FOWT is investigated for validation of the improved gradient-based retrieval algorithm and the proposed discretization approach. In addition, the ECs of 10-, 100-, and 1 000-year RPs in the South China Sea are established. The long-term response extremes are obtained and investigated. The *N*-year extreme response of the structure obtained via IFORM are all located inside the ECs, which demonstrates that the selection of design sea conditions based on the method proposed in this paper may result in a more economical finding than the EC method. Numerical studies show that the proposed approach can be used to calculate the long-term structural response of general offshore floating structures without requiring analytically expressed RAOs.

Funding Supported by the National Natural Science Foundation of China (Grant Nos. 52088102 and 51879287), and National Key Research and Development Program of China (Grant No. 2022YFB2602301).

Competing interest The authors have no competing interests to declare that are relevant to the content of this article.

References

Baarholm GS, Moan T (2000) Estimation of nonlinear long-term extremes of hull girder loads in ships. Marine Structures 13(6): 495-516. https://doi.org/10.1016/s0951-8339(00)00060-5

Battjes JA (1972) Long-term wave height distributions at seven stations around the British Isles. Deutsche Hydrographische Zeitschrift 25(4): 179-189. https://doi.org/10.1007/bf02312702

Beshbichi OE, Rødstøl H, Xing Y, Ong MC (2022) Prediction of long-term extreme response of two-rotor floating wind turbine concept using the modified environmental contour method. Renewable Energy 189: 1133-1144. https://doi.org/10.1016/j.renene.2022.02.119

Bruserud K, Haver S, Myrhaug D (2018) Joint description of waves and currents applied in a simplified load case. Marine Structures 58: 416-433. https://doi.org/10.1016/j.marstruc.2017.12.010

Castellon DF, Fenerci A, Øiseth O, Petersen ØW (2022) Investigations of the long-term extreme buffeting response of long-span bridges using importance sampling Monte Carlo simulations. Engineering Structures 273: 114986-114986. https://doi.org/10.1016/j.engstruct.2022.114986

Chen DS, Feng XY, Li ZQ, Chen JF (2023) Long-term extreme responses of torsional moments at two-directional hinges for moored very large floating structures. Ocean Engineering 290: 116330-116330. https://doi.org/10.1016/j.oceaneng.2023.116330

Clarindo G, Guedes Soares C (2024) Environmental contours of sea states by the I-FORM approach derived with the Burr-Lognormal statistical model. Ocean Engineering 291: 116315. https://doi.org/10.1016/j.oceaneng.2023.113959

Du X, Sudjianto A, Chen W (2004) An integrated framework for optimization under uncertainty using inverse reliability strategy. Journal of Mechanical Design 126(4): 562-570. https://doi.org/10.1115/1.1759358

Ewans K, Jonathan P (2014) Evaluating environmental joint extremes for the offshore industry using the conditional extremes model. Journal of Marine Systems 130: 124-130. https://doi.org/10.1016/j.jmarsys.2013.03.007

Farnes KA, Moan T (1993) Extreme dynamic, non-linear response of fixed platforms using a complete long-term approach. Applied Ocean Research 15(6): 317-326. https://doi.org/10.1016/0141-1187(93)90001-e

Fontaine E, Orsero P, Ledoux A, Nerzic R, Prevosto M, Quiniou V (2013) Reliability analysis and response based design of a moored FPSO in West Africa. Structural Safety 41: 82-96. https://doi.org/10.1016/j.strusafe.2012.08.002

Giske FIG, Kvåle KA, Leira BJ, Øiseth O (2018) Long-term extreme response analysis of a long-span pontoon bridge. Marine Structures 58: 154-171. https://doi.org/10.1016/j.marstruc.2017.11.010

Giske FIG, Leira BJ, Øiseth O (2017) Full long-term extreme response analysis of marine structures using inverse FORM. Probabilistic Engineering Mechanics 50: 1-8. https://doi.org/10.1016/j.probengmech.2017.10.007

Haver S (1985) Wave climate off northern Norway. Applied Ocean Research 7(2): 85-92. https://doi.org/10.1016/0141-1187(85)90038-0

Haver S, Winterstein SR (2008) Environmental contour lines: A method for estimating long term extremes by a short term analysis. Transactions-Society of Naval Architects and Marine Engineers. 116: 116-127 https://doi.org/10.5957/smc-2008-067

Krogstad HE (1985) Height and period distributions of extreme waves. Applied Ocean Research 7(3): 158-165. https://doi.org/10.1016/0141-1187(85)90008-2

Li H, Foschi RO (1998) An inverse reliability method and its application. Structural Safety 20(3): 257-270. https://doi.org/10.1016/s0167-4730(98)00010-1

Li L, Yuan ZM, Gao Y, Zhang XS, Tezdogan T (2019) Investigation on long-term extreme response of an integrated offshore renewable energy device with a modified environmental contour method. Renewable Energy 132: 33-42. https://doi.org/10.1016/j.renene.2018.07.138

Li Q, Gao Z, Moan T (2017) Modified environmental contour method to determine the long-term extreme responses of a semi-submersible wind turbine. Ocean Engineering 142: 563-576. https://doi.org/10.1016/j.oceaneng.2017.07.038

Liao ZK, Zhao YL, Dong S (2022). Estimating design loads for floating structures using environmental contours. Journal of Marine Science and Application 21(3): 114-127. https://doi.org/10.1007/s11804-022-00282-x

Longuet-Higgins MS (1975) On the joint distribution of the periods and amplitudes of sea waves. Journal of Geophysical Research 80(18): 2688-2694. https://doi.org/10.1029/jc080i018p02688

Lystad TM, Fenerci A, Øiseth O (2020) Buffeting response of long-span bridges considering uncertain turbulence parameters using the environmental contour method. Engineering Structures 213: 110575. https://doi.org/10.1016/j.engstruct.2020.110575

Mackay E, Hauteclocque GD (2023) Model-free environmental contours in higher dimensions. Ocean Engineering 273: 113959-113959. https://doi.org/10.1016/j.oceaneng.2023.113959

Naess A (1984) Technical note: On the long-term statistics of extremes. Applied Ocean Research 6(4): 227-228. https://doi.org/10.1016/0141-1187(84)90061-0

Naess A, Moan T (2012) Stochastic dynamics of marine structures. Cambridge University Press, Cambridge. ISBN: 9781139021364

Ochi MK (1998) Ocean waves: the stochastic approach. Cambridge University Press

Sagrilo L, Naess A, Doria AS (2011) On the long-term response of marine structures. Applied Ocean Research 33(3): 208-214. https://doi.org/10.1016/j.apor.2011.02.005

Vanem E (2016) Joint statistical models for significant wave height and wave period in a changing climate. Marine Structures 49: 180-205. https://doi.org/10.1016/j.marstruc.2016.06.001

Vázquez-Hernández AO, Ellwanger GB, Sagrilo LVS (2011) Long-term response analysis of FPSO mooring systems. Applied Ocean Research 33(4): 375-383. https://doi.org/10.1016/j.apor.2011.05.003

Wang YG (2020) A novel environmental contour method for predicting long-term extreme wave conditions. Renewable Energy 162: 926-933. https://doi.org/10.1016/j.renene.2020.08.112

Winterstein SR, Ude TC, Cornell CA, Bjerager P, Haver S (1993) Environmental parameters for extreme response Inverse FORM with omission factors. ICOSSAR-93, Innsbruck, 551-557